ADVANCED OPTICAL MATERIALS
www.advopticalmat.de

Unveiling the Transformation from Aggregation-Caused Quenching to Encapsulation-Induced Emission Enhancement for Improving the Photoluminescence Properties and Detection Performance of Conjugated Polymer Material in Multiple States

Sameer Hussain, Xi Chen, Yingying Gao, Huijia Song, Xuemeng Tian, Yulian He, Ansar Abbas, Mohammad Adil Afroz, Yi Hao, and Ruixia Gao**

High hydrophobicity of π-extended conjugated polymers (CPs) adversely affects their photoluminescence quantum yield (PLQY) in water and hydrogel/solid state via an unsolicited aggregation-caused quenching (ACQ) process which ultimately hampers their sensing and imaging performance. Herein, an efficient strategy is presented to suppress and transform such ACQ process into an encapsulation-induced emission enhancement (EIEE) effect through facile preparation of CP/Pluronic F-127 fluorescent hybrid micelles and hydrogel. As a proof-of-concept, successful encapsulation of polyfluorene derivative PF-DBT-Im into F-127 micelles not only displays an improved PLQY (≈200% increment) in water/hydrogel state but also delivers unique and augmented sensing responses toward the emerging pollutants tetracyclines taken as model analyte, validating the superiority of EIEE-active hybrid micellar systems over ACQ suffering PF-DBT-Im aggregates. The established method not only provides a facile solution to circumvent ACQ problem existing in low water dispersible CPs but also endorses an enhanced, simplified sensing system for visual and on-site detection of analytes with likely futuristic applications in biomedicine and solid-state optoelectronics.

1. Introduction

As a pioneering class of metal-free luminescent organic materials, conjugated polymers (CPs) are widely employed in the domains of optoelectronics,[1–3] fluorescent sensors,[4–7] and bioimaging[8,9] owing to their numerous astonishing optical features. Moreover, the amplified signal response owing to the unique "molecular-wire effect"[4] certifies them as superior fluorescent probes over small monomeric sensors. Despite these promising characteristics, the long-lasting problem of aggregation-caused quenching (ACQ) via strong π–π stacking[10–12] severely impacts the optical performance of CP-based probes, especially the photoluminescence quantum yield (PLQY) in aqueous media and prominently in hydrogel/solid state. This is thanks to the discovery[13–15] of aggregation-induced emission (AIE) process typically perceived in rotor molecules such as tetraphenylethylene, which can assist in transforming ACQ molecules into AIE luminogens (AIEgens). Such alteration undoubtedly provides a potential solution to impede the ACQ problem in CPs;[14–17] however, on the basis of strict molecular designing strategies. Other conventional methods to beat ACQ include, for instance, grafting[18,19] of non-conjugated moieties, employment[20] of surfactant stabilizers, sandwich-type encapsulation[21] of CPs, and/or the incorporation[22] of charged

S. Hussain, X. Chen, Y. Gao, X. Tian, A. Abbas, Y. Hao, R. Gao
School of Chemistry
Xi'an Jiaotong University
Xi'an 710049, P. R. China
E-mail: haoyi8904@xjtu.edu.cn; ruixiagao@xjtu.edu.cn
H. Song
Department of Urology
Second Affiliated Hospital of Xi'an Jiaotong University
Xi'an 710004, P. R. China
Y. He
University of Michigan-Shanghai Jiaotong University Joint Institute
Shanghai Jiaotong University
200240 Shanghai, P. R. China
M. A. Afroz
Department of Physics
Indian Institute of Technology Roorkee
Roorkee, Haridwar, Uttarakhand 247667, India
Y. Hao
School of Pharmacy
Health Science Center
Xi'an Jiaotong University
Xi'an 710061, P. R. China
The ORCID identification number(s) for the author(s) of this article can be found under https://doi.org/10.1002/adom.202202851

DOI: 10.1002/adom.202202851

groups along the side chains. However, such alterations remain incompetent in adequately improving the emissive properties of CPs, especially in solid state. Similarly, embedding light harvesting CPs into a gel skeleton to obtain the high-performance emissive hydrogel remains a difficult task for material scientists due to the strong π–π stacking of CPs. Though few sincere efforts[23–26] have been made in the past to acquire CP-based fluorescent hydrogels, they have certain limitations. Thus, the exploration of an alternative method resembling AIE to both inhibit ACQ effect and enhance the overall PLQY of low water dispersible CPs without employing tedious synthetic procedures would be of great significance. Recently, Yoshizawa et al.[27] revealed that the emission of metal complexes could be enhanced by encapsulating them into aromatic micelles. Liu's pioneering research group[28] demonstrates the fabrication of highly photoluminescent supramolecular nanoparticle system by encapsulating FRET pair of dithienylethene derivative and β-cyclodextrin-functionalized Ru complex into Pluronic F-127 matrix via hydrophilic–hydrophobic interactions. Encouraging from these reports, we proposed an encapsulation-induced emission enhancement (EIEE) of CP material through facile preparation of fluorescent hybrid micelles and hydrogel using F-127 as encapsulating material. This led to the improvement in PLQY of CP and the resulting hybrid material can be utilized for augmented detection of suitable analytes in aqueous media and gel state.

Antibiotics, among the most common pharmaceutical products used worldwide for combatting infections, are considered as a major source of environmental pollutants.[29,30] Tetracycline antibiotics (TCs) such as chlortetracycline (CTC), doxycycline (DOX), oxytetracycline (OTC), and tetracycline (TET) are broad-spectrum antibiotics employed for curing pathogenic infections in both human and animals. However, the abuse of TCs especially as feed additives can pose adverse effects on human health through food chain transmission.[31–34] To date, several types of materials and techniques have been established[30,32,35–37] for monitoring TCs, yet most of them are costly, sophisticated, less sensitive, and/or remained unviable for visual on-site detection. In the view of growing concerns associated with both environment as well as public health, the precise and rapid identification of TCs using smart sensing systems is highly imperative. Thus, TCs are chosen as analytes of interest in the current study for signifying the superiority of designed EIEE-active system.

Herein, we demonstrate the unusual phenomenon of EIEE in fluorescent hybrid micelles and hydrogel composed of fluorescent CP PF-DBT-Im–a derivative of polyfluorene and amphiphilic biopolymer Pluronic F-127 for amplified monitoring of TCs (**Scheme 1**). Above critical micelle concentration (c > cmc), the non-toxic Pluronic F-127 molecules can easily encapsulate the hydrophobic PF-DBT-Im into inner space of micelles in a highly ordered fashion and therefore enhance its overall PLQY (Φ) from 0.10 to 0.29 due to inhibition of π–π stacking and reduction of non-radiative transitions, endorsing the successful transformation of ACQ-suffered PF-DBT-Im nanoaggregates into vibrant EIEE-active fluorescent micelles. Above critical gelation concentration (c > cgc) of F-127, the association of micelles led to the formation of room-temperature stable, highly fluorescent, and injectable EIEE-active hydrogel with an improved PLQY (Φ) of 0.30. Finally, the as-prepared EIEE-active micelles and hydrogel were positively employed for amplified and highly specific detection of TCs. Interestingly, such EIEE-active micelles displayed an enhanced response toward TCs via synergistic effect of photo-induced electron transfer (PET), inner-filter effect (IFE), and long-range exciton transport, in contrast with PF-DBT-Im random aggregates which displayed a less sensitive response primarily from IFE and short-range exciton migration. Moreover, through simple gel-to-sol transition and consequent fluorescent quenching, the EIEE-active hydrogel system endorses a convenient and reliable platform for attaining visual and on-site TCs detection at desirable places.

2. Results and Discussion

To demonstrate the phenomenon of EIEE for curbing ACQ affect in conjugated polymer material, our previously synthesized[38] (Scheme S1 and Figure S1, Supporting Information) cationic CP PF-DBT-Im (**Figure 1**a) was chosen as a model material as it exhibited a poor water solubility, a low PLQY (Φ = 0.10) in water, and color-tunable emission. On the other hand, various Pluronics (Figure 1b) with amphiphilic triblock copolymer structures consisting of poly(ethylene oxide)-poly(propylene oxide)-poly(ethylene oxide) (PEO_m-PPO_n-PEO_m) were employed as encapsulating materials, because, they are biocompatible materials that exhibit strong tendency[28,39–42] to solubilize hydrophobic molecules and encapsulate them into the hydrophobic cores of micelles. On introducing a fixed concentration (10 μM) of PF-DBT-Im to the solutions of different Pluronics kept under stirring in water above their cmc, fluorescence enhancement (λ_{ex} = 380 nm) of variable magnitudes was observed (Figure 1c) at both the emission peaks of PF-DBT-Im, that is, 420 and 630 nm assigned to π–π* transition[38] of fluorene and dithienylbenzothiadiazole (DBT) segments along the backbone, respectively. The concentration of different Pluronics above their respective cmc[43] was fixed according to the maximum enhancement of fluorescence. To visualize and quantify the EIEE effect, the changes in the solution emission color and PLQY values determined for PF-DBT-Im in the presence of several Pluronics above their cmc values were studied as shown in Figure 1d. Pluronic F-127 displayed a maximum fluorescence enhancement with ≈200% increment in overall PLQY of PF-DBT-Im (Φ = 0.29). The emission enhancement and the improved PLQY could be attributed to a better solubilization resulting from the encapsulation of hydrophobic PF-DBT-Im into the core of micelles in a spatially confined zone.[44] Such regular spatial confinements not only assist in enhancing the PLQY through inhibition of π–π stacking and reduction of non-radiative transitions[45,46] but also facilitate a more sensitive detection through the more favorable long-range exciton transport[41,47,48] along the much closer polymer chains. Note that the solubilization power of Pluronics strongly depends[43,49] on their molecular weights (M_w) as well as the hydrophilic–lipophilic balance (HLB), that is, a better solubilization is observed generally in Pluronic possessing a higher M_w and a lower HLB. Moreover, at fixed HLB values, Pluronic possessing higher M_w renders better solubilization.[43,49] Pluronics F-127 and F-108 exhibit higher M_w compared to other Pluronics used in current study and consequently promote a more efficient solubilization of PF-DBT-Im inside the micelles; and therefore, enhance PLQY considerably. On the other hand, Pluronics L-35

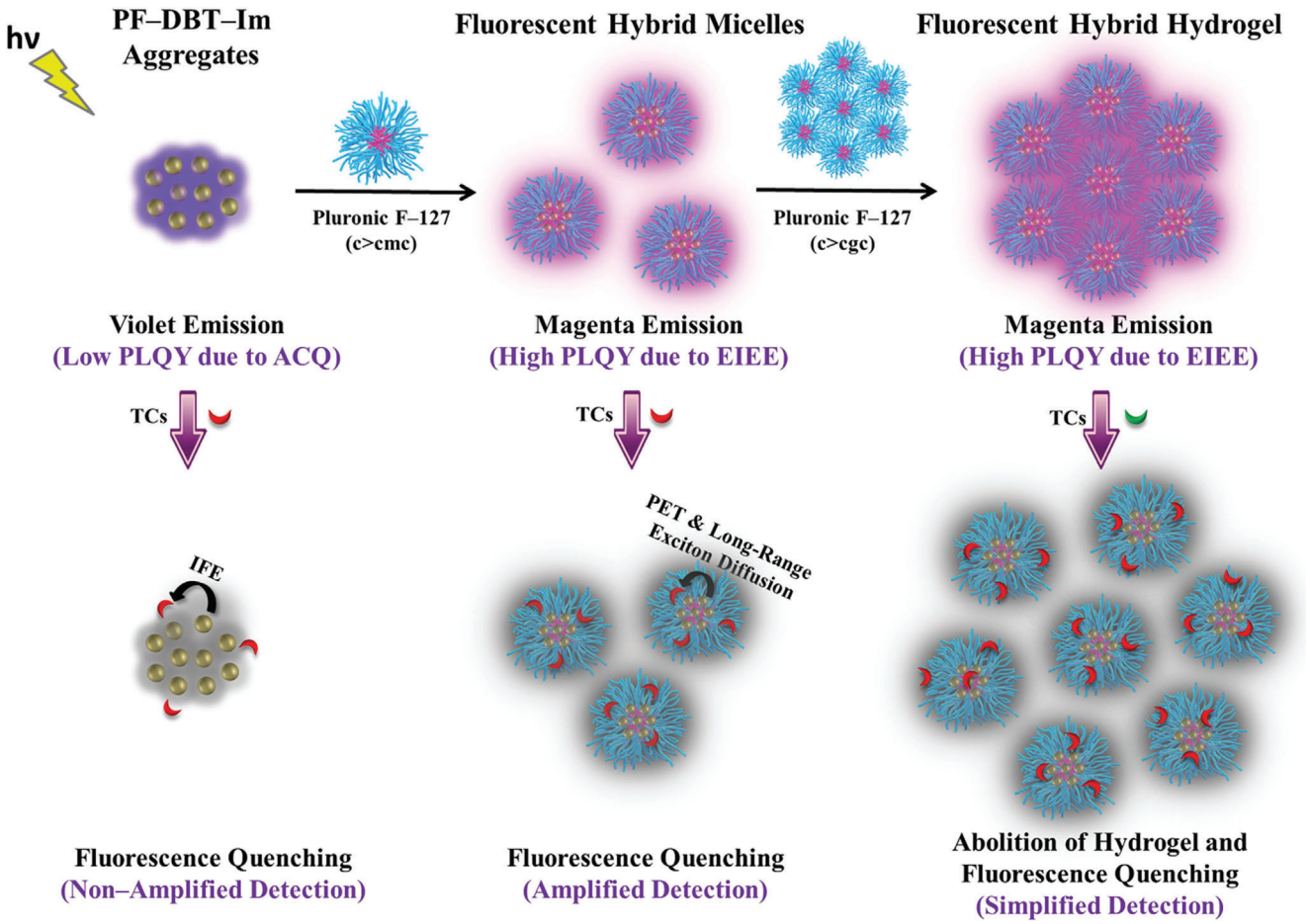

Scheme 1. Schematic illustration of the preparation of EIEE-active hybrid micelles and hydrogel using conjugated polymer PF-DBT-Im and Pluronic F-127 for augmented and simplified detection of emerging pollutants tetracyclines.

and F-127 possess the same HLB (18-23) values, while a higher PLQY value was observed with the latter owing to its higher M_w value. Similarly, Pluronics F-68 and F-108 also hold the same HLB (>24) values, while a higher PLQY was observed with F-108 due to a greater M_w of F-108. Noteworthy, F-127 is the only commercially available Pluronic that exhibits the least HLB value and the highest M_w; therefore appearing as the best for solubilizing PF-DBT-Im in water. The effect of dopant (PF-DBT-Im) concentration as well as encapsulating material (Pluronic-F127) on the EIEE process were also studied (Figure 1e). As a result, Pluronic-F127 with 10 μM concentration turned out to be sufficient for solubilizing the low concentrations (5–10 μM) of polymer and causing maximum emission enhancement (λ_{em} = 420 nm). However, at higher polymer concentrations (20–40 μM), a higher concentration (50 μM) of Pluronic F-127 was required to competently encapsulate the hydrophobic polymer and attain proficient EIEE. Nevertheless, a substantial emission enhancement was observed (Figure 1f) at variable concentrations of PF-DBT-Im, which confirms the adaptability of EIEE process even at higher polymer concentrations where the ACQ effect is prone to be significant.

To investigate the encapsulation process, the morphology of PF-DBT-Im/Pluronic F-127 EIEE-active micelles was studied using scanning electron microscopy (SEM), transmission electron microscopy (TEM), and fluorescence microscopy. SEM images indicate that PF-DBT-Im exhibited as spherical nanoaggregates in native state (**Figure 2**a), whereas F-127 displayed clusters of micelles (Figure 2b) in aqueous solution. In the presence of PF-DBT-Im, the micelles are transformed into highly ordered "divergent" structures (Figure 2c) owing to self-association of relatively larger size polymer encapsulated micelles. TEM image (Figure 2d) of PF-DBT-Im/Pluronic F-127 hybrid micelles indicates the presence of core–shell morphology confirming the successful encapsulation of polymer into the hydrophobic core of micelles. Besides, the elemental mapping results also support the core–shell structure and successful encapsulation of polymer by F-127 micelles (Figure 2g). Furthermore, the fluorescence property of EIEE-active micelles was confirmed via fluorescence microscopy under UV (Figure 2e) and green light (Figure 2f) irradiation. The micelles displayed a bright magenta color emission under UV light source from the combined emission of fluorene and DBT segments, whereas a pure red fluorescence signal was observed under the green light source owing to the selective excitation of only DBT units. This is consistent with the fluorescence spectroscopic results and further validated the fluorescence property of hybrid micelles. To check the flexibility of EIEE affect, two more

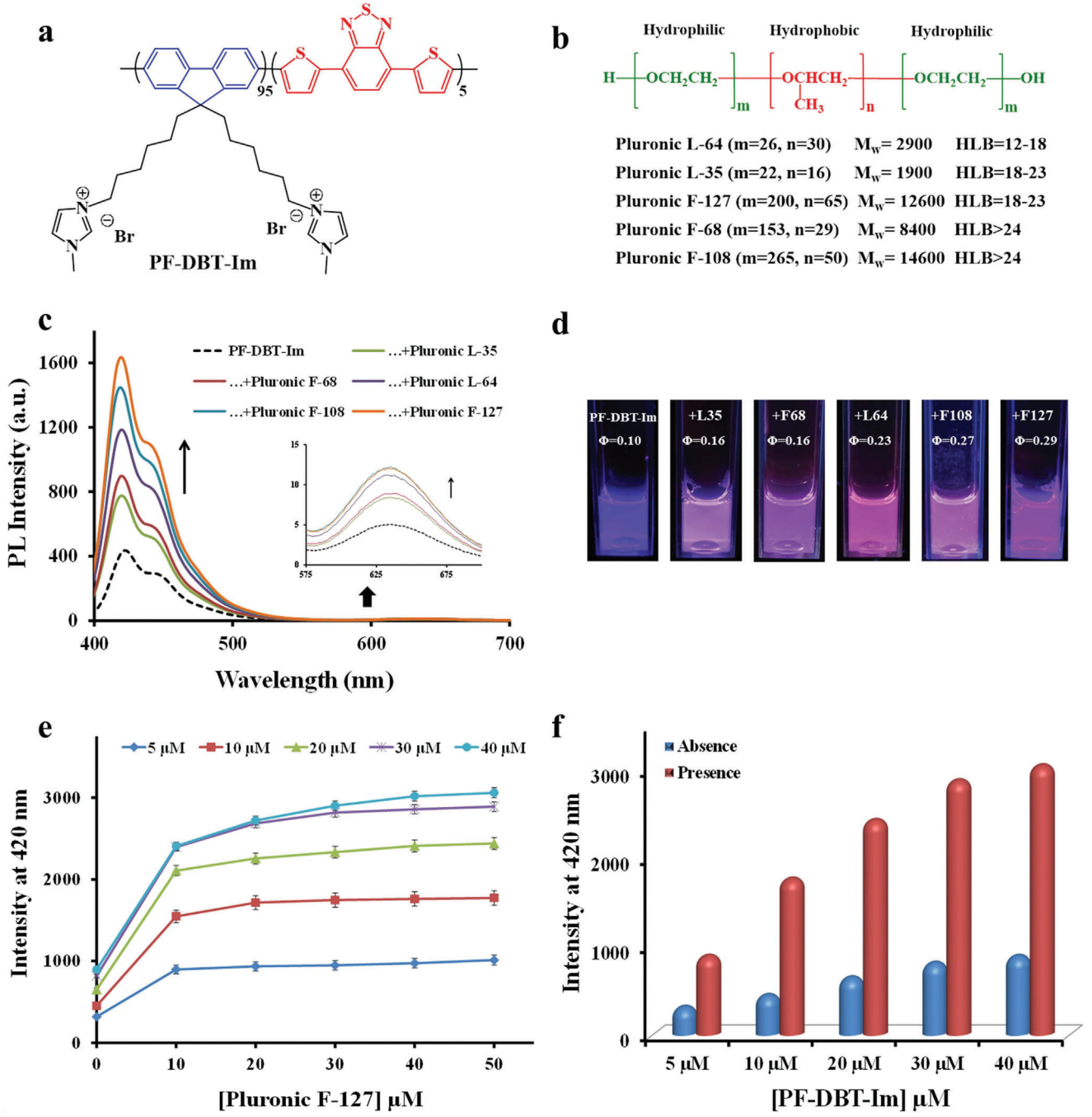

Figure 1. Chemical structure of a) conjugated polymer PF-DBT-Im and b) different Pluronics used in the study. c) Emission enhancement and d) change in color of PF-DBT-Im (10 μM) solution under UV light with various Pluronics at 37 °C. The concentration of each Pluronic was above their cmc (L-35 [5.5 mM], F-68 [0.6 mM], L-64 [0.8 mM], F-127 [10 μM], and F-108 [100 μM]). e) Effect of various Pluronic F-127 concentrations on the emission enhancement of PF-DBT-Im (5–40 μM). f) Maximum emission enhancement observed at variable concentrations of PF-DBT-Im in the absence and presence of Pluronic F-127 (50 μM).

low water dispersible CPs, that is, PF-DBT-COONa and PF-BT-Im were synthesized (Figures S2 and S3, Supporting Information) and studied. Interestingly, both the CPs demonstrate significant improvement in their PLQY after forming fluorescent hybrid micelles (Figure S4, Supporting Information), affirming versatility of EIEE effect for low water dispersible CPs.

To demonstrate the superiority of EIEE-active PF-DBT-Im/Pluronic F-127 micelles over ACQ affected PF-DBT-Im aggregates in the arena of detection, sensing studies were performed with various tetracycline antibiotics in 10 mM HEPES buffer (pH = 7.4). It is clear from **Figure 3**a–d that all four TCs demonstrate substantial fluorescence quenching toward

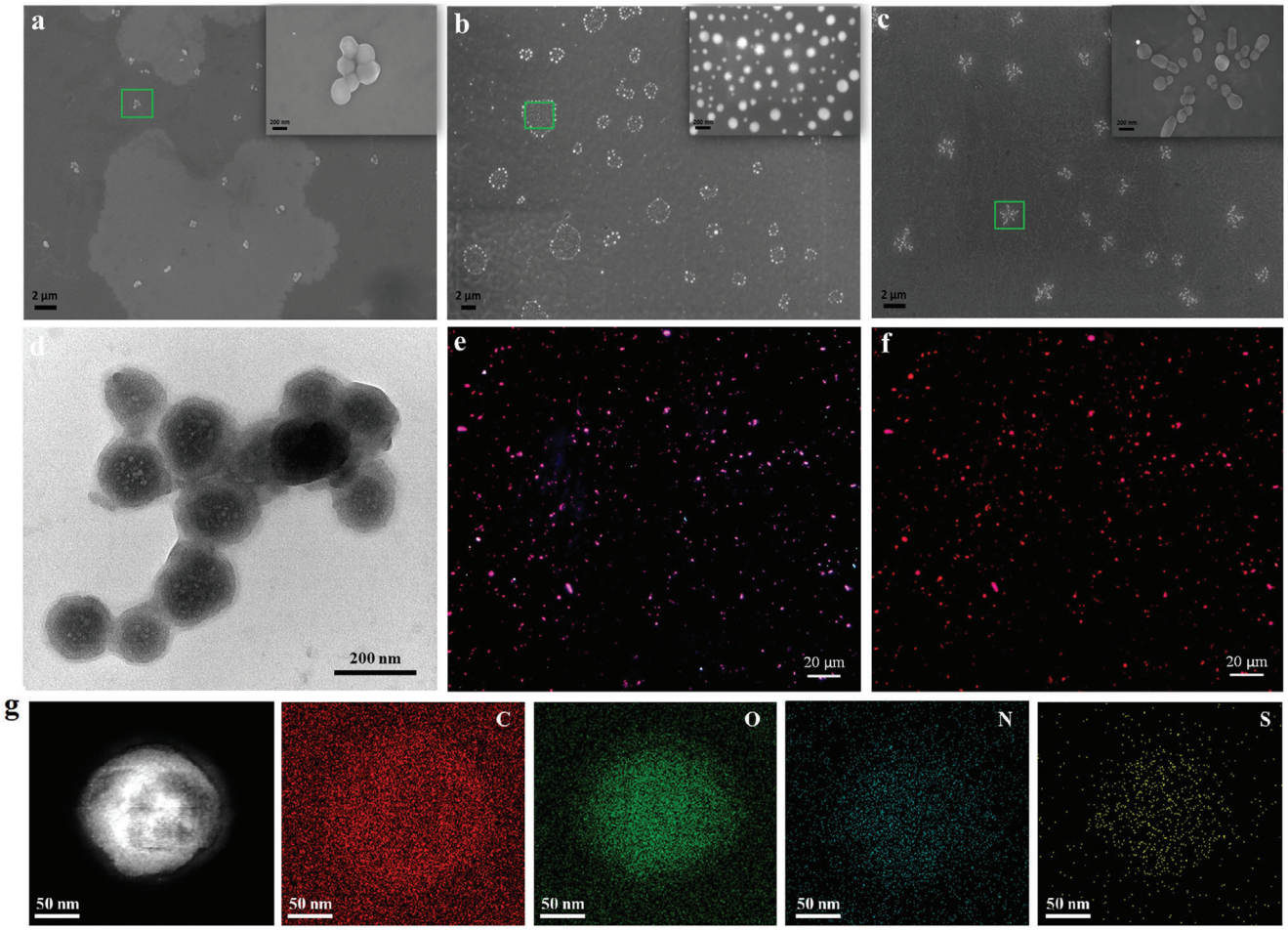

Figure 2. SEM images of a) PF-DBT-Im (10 μM), b) Pluronic F-127 (10 μM), and c) PF-DBT-Im/Pluronic F-127 (10 μM/10 μM), respectively. d) TEM image of PF-DBT-Im/Pluronic F-127 hybrid micelles. Fluorescence microscopic images of hybrid micelles under irradiation of e) UV and f) green light. g) Energy-dispersive X-ray spectroscopy (EDX) mapping of PF-DBT-Im/Pluronic F-127 EIEE-active hybrid micelle. The presence of element O indicate Pluronic F-127 whereas, elements N and S confirm the successful encapsulation of polymer by micelle.

EIEE-active micelles with reasonable Stern–Volmer quenching constant (K_{sv}) values of 165 342 M^{-1} (CTC), 98 278 M^{-1} (OTC), 97 361 M^{-1} (DOX), and 73 719 M^{-1} (TET), respectively, confirming notable sensitivity of hybrid micellar system for TCs. Moreover, the disappearance of magenta color was obvious under UV lamp excitation, facilitating visual naked-eye detection. The detection limits (Figures S5–S8, Supporting Information) obtained for CTC (129 ppb), OTC (154 ppb), DOX (159 ppb), and TET (192 ppb), respectively, clearly indicate the advantage of the hybrid system in monitoring traces of TCs. Competitive studies (Figure 3e,f) with several other antibiotics (streptomycin, lincomycin, ampicillin, chloramphenicol, sulfamethoxazole, erythromycin, and sulfadiazine), metal ions (Cu^{2+}, Cd^{2+}, Co^{2+}, and Mg^{2+}), anions (Cl^-, SO_4^{2-}, CH_3COO^-, CO_3^{2-}, and $C_2O_4^{2-}$) and amino acids (histidine, cysteine, valine, tryptophan, and isoleucine) indicate exclusive selectivity of EIEE-active micellar system, which is a prerequisite for it to be utilized under realistic conditions. On the contrary, PF-DBT-Im nanoaggregates displayed a (Figure S9, Supporting Informatiion) less fluorescence quenching response, less significant color changes, and comparatively lower K_{sv} values of 129 835 M^{-1} (CTC), 42 323 M^{-1} (OTC), 63 892 M^{-1} (DOX), and 43 110 M^{-1} (TET), respectively, signifying supremacy of EIEE-active hybrid micellar system over PF-DBT-Im aggregates in detecting tetracycline antibiotics.

To comprehend the reason behind the observed ultrasensitivity and exclusive selectivity and to shed light on the underlying sensing mechanism, the excitation/emission spectrum of PF-DBT-Im/Pluronic F-127 was compared with the absorption spectra of the antibiotics used. As shown in **Figure 4**a, certain overlapping was observed between the emission/excitation spectra of EIEE-active micelles and the absorption spectra of TCs, indicating the possibility of either Förster resonance energy transfer (FRET) or inner-filter effect (IFE). FRET[50] is a non- radiative process which implicates the transfer of excited state energy of fluorophore to quencher whereas IFE[37] deals with absorption of excitation and/or emission energy of fluorophore by the quencher molecule. Time-resolved fluorescence spectroscopy (Figure 4b) affirms that the lifetime of EIEE-active micelles (2.16 ns) only changed slightly with TCs (CTC-1.82 ns, OTC-1.97 ns, DOX-2.11 ns, and TET-2.10 ns), eluding the chance of capable FRET, which would otherwise show substantial decrement. Thus, the possibility of IFE was studied using the standard IFE

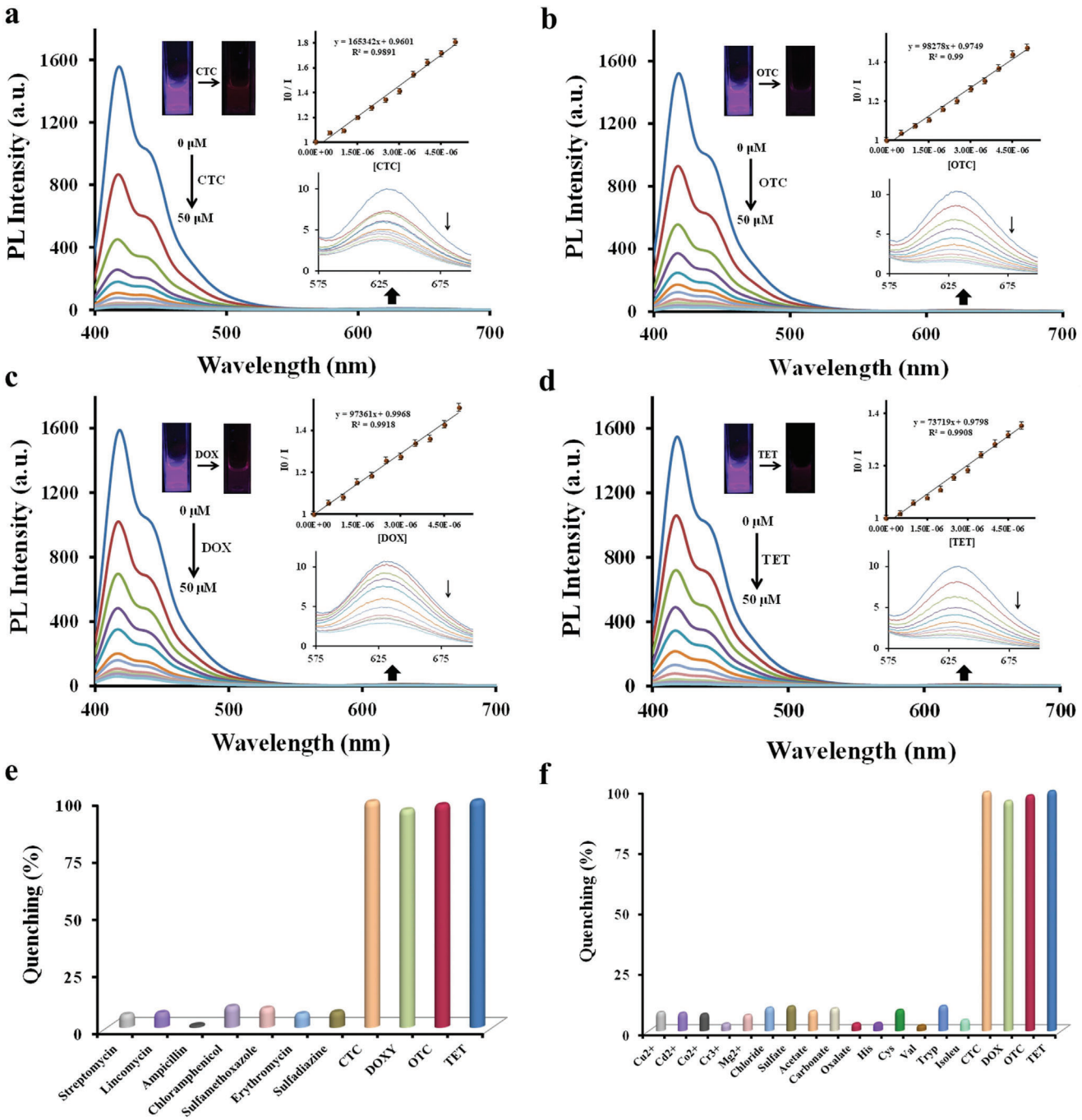

Figure 3. Emission spectra of PF-DBT-Im/Pluronic F-127 (10 μM/10 μM) with increasing concentration of a) CTC, b) OTC, c) DOX, and d) TET, respectively. Inset: Corresponding change in emission color of solution under UV light and K_{sv} plot. Selectivity plots with e) different antibiotics and f) other interfering analytes.

correction equation[37] and the corresponding absorption spectra of EIEE-active micelles with variable concentration of TCs are presented in Figure S10, Supporting Information. The obtained correction plots (Figure S11, Supporting Information) suggest that IFE only plays a minor role (≈6–9%) in the quenching process and further hints at the involvement of some additional mechanisms. Besides, the role of IFE was found to be major (25–75%) in the detection of TCs using PF-DBT-Im nanoaggregates (Figures S12 and S13, Supporting Information) because the emission/excitation of PF-DBT-Im could also overlap efficiently with the absorption of TCs, and the lifetime changes were insignificant (Figure S14, Supporting Information). Such a notable IFE process and low sensitivity in the case of PF-DBT-Im nanoaggregates indicates the absence of any possible interactions between probe and the TCs. Note that the interactions between the probe and analyte are vital for boosting the

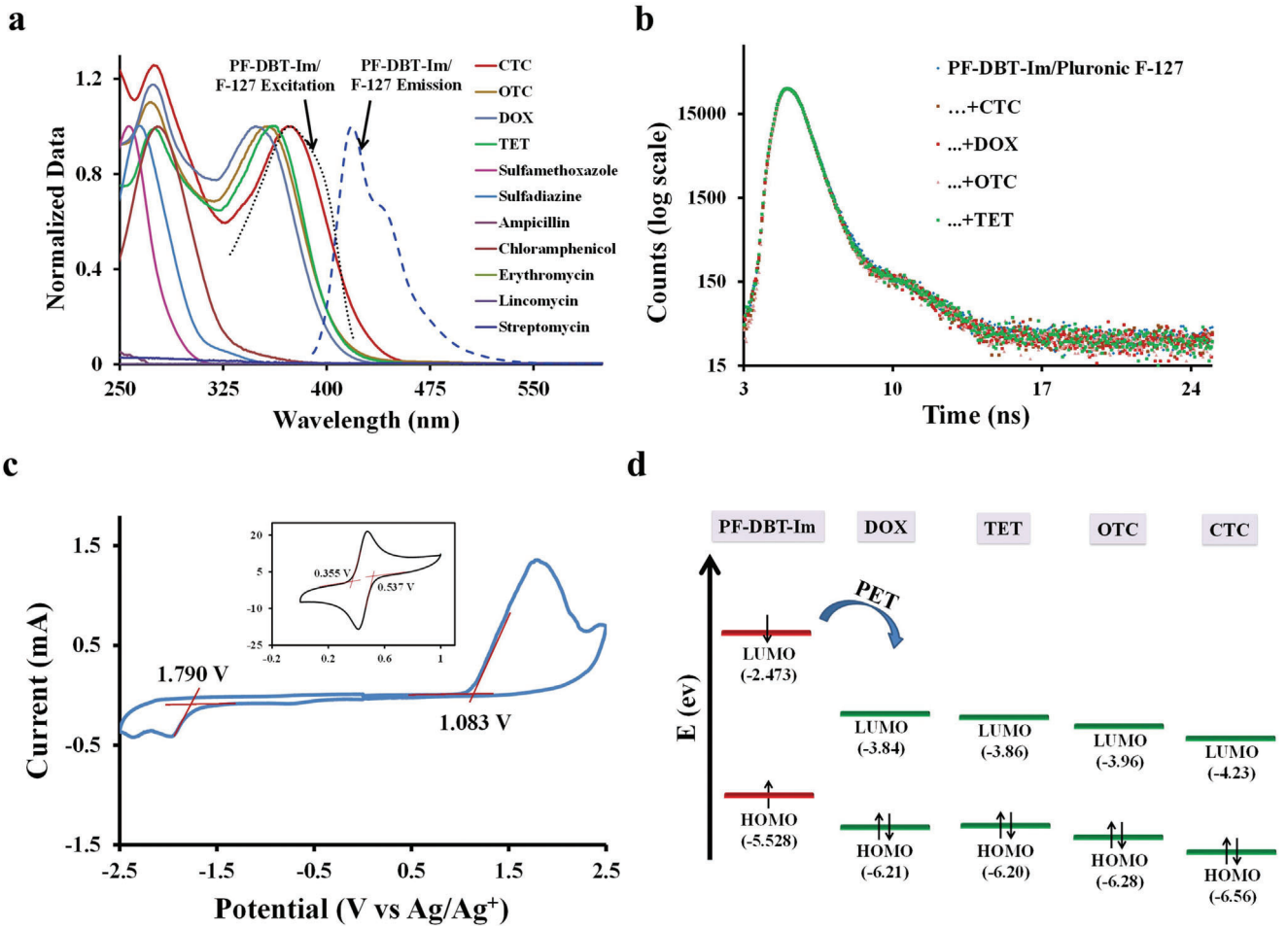

Figure 4. a) Spectral overlap between excitation/emission spectra of PF-DBT-Im/Pluronic F-127 and absorption spectra of various antibiotics used. b) Change in lifetime decay of PF-DBT-Im/Pluronic F-127 with different TCs. c) Cyclic voltammogram (CV) of PF-DBT-Im on a glassy carbon electrode in CH_3CN. Inset: CV of ferrocene as reference. d) Pictorial illustration of photo-induced electron (PET) transfer from LUMO of PF-DBT-Im to LUMO of TCs.

fluorescence responses and attaining an amplified detection. Conjugated polymers are semi-conducting materials that exhibit reasonable band gaps and favor numerous[37,51,52] electron transfer processes with the analytes. To elucidate the role of electron transfer in the quenching process, highest occupied molecular orbital (HOMO) and lower unoccupied molecular orbital (LUMO) values of PF-DBT-Im were determined via cyclic voltammetry (Figure 4c), while HOMO/LUMO values of TCs were acquired from the literature.[35] As illustrated in Figure 4d, there is a strong possibility of photo-induced electron transfer (PET) from LUMO of polymer to LUMO of TCs, resulting in significant fluorescence quenching. However, PET is a distance-dependent process and requires favorable interactions between the probe and the analyte to induce significant changes. TCs bearing numerous hydrogen bonding active groups (–OH, –NH) could easily come into proximity with EIEE-active micelles through favorable hydrogen bonding interactions with hydroxyl groups of Pluronic F-127 and subsequently cause enhanced fluorescence quenching via the strong PET process. Furthermore, the spatial confinement of polymer inside the micelles with an enhanced PLQY provides an appropriate environment for long-range exciton diffusion[47,48] of quencher molecules to ultimately deliver ultrasensitive fluorescence quenching response. In addition, the outer hydrophilic shell of PEO provides a protective environment to reduce the influence of external interference on PF-DBT-Im which is already embedded inside the core of micelles. Besides, owing to the absence of any favorable binding between PF-DBT-Im aggregates and TCs, the fluorescence response could not be governed by PET process. Thus, favorable hydrogen bonding interactions mediated PET along with rapid long-range exciton diffusion could synergistically augment the detection efficiency of EIEE-active hybrid micelles toward TCs in contrast to the counterpart PF-DBT-Im nanoaggregates, which could only facilitate IFE.

Solid-state fluorescent materials in native or hybrid state are auspicious and remain desirable in the areas of optoelectronics,[53,54] sensors,[55,56] and other biomedical[15,55] applications. Among such materials, luminescent hybrid hydrogels[24,57–60] as injectable scaffolds are extensively demanded for optical sensing, imaging, wound healing, and so on. To encounter the prevailing issues[23–26] in the development of CP based fluorescent hydrogels, we present a straightforward strategy to prepare PF-DBT-Im based EIEE-active hydrogel with

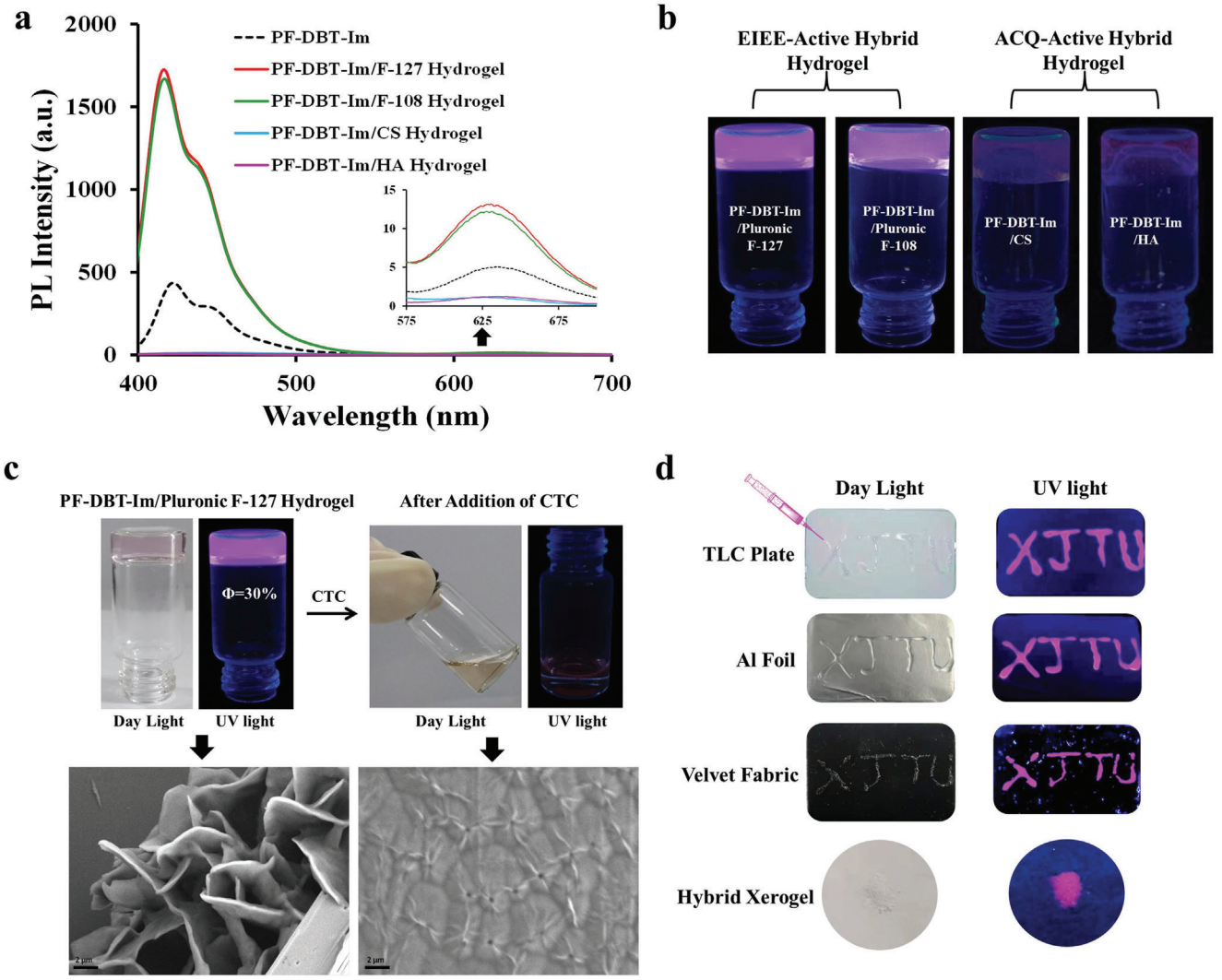

Figure 5. a) Changes in the emission spectra of PF-DBT-Im after forming hydrogels with 20% w/v Pluronic F-127, 20% w/v Pluronic F-108, 5% w/v CS, and 5% w/v CS HA, respectively. b) Corresponding images of hydrogels under UV light irradiation. c) Abolition, fluorescence quenching, and SEM images of EIEE-active PF-DBT-Im/Pluronic F-127 hydrogel upon addition of CTC (100 μM). d) Pictures of PF-DBT-Im/Pluronic F-127 hydrogel cast on various substrates and corresponding xerogel under day light and UV light.

enhanced PLQY and without any loss of original spectral characteristics, employing Pluronics F-127 and F-108 as carrier. Highly fluorescent and thermo-responsive EIEE-active hydrogels were obtained by simple doping of PF-DBT-Im (10 μM) to 20% w/v Pluronic F-108 and F-127 solutions in water separately at low temperature (≈5 °C), followed by settling the respective solutions to room temperature. Pluronics F-108 and F-127 were selected considering their excellent gelation ability at room temperature and the high PLQY of PF-DBT-Im in respective micelles. Both hydrogels displayed significant emission enhancement (**Figure 5**a) and bright fluorescence color under UV light irradiation (Figure 5b). The PLQY of EIEE-active PF-DBT-Im/Pluronic F-108 ($\Phi = 0.28$) and PF-DBT-Im/Pluronic F-127 ($\Phi = 0.30$) hydrogels were found to be slightly higher than their corresponding micelles because Pluronics hydrogel are usually formed through systematic association of micelles over increasing temperature (>10 °C) when hydrophobic interactions become favorable among PPO domains.[43,49] The hydrogels remain stable at room temperature and transform into solution if kept in refrigerator because the hydration layer generally surrounds Pluronic micelles through hydrogen bonding at lower temperatures and will be disrupted at elevated temperatures owing to the desolvation of hydrophilic chains. To confirm whether gelation through regular micellar associations are necessary to realize EIEE effect of CP in the hydrogel, PF-DBT-Im was doped with two other most common biopolymers, that is, hyaluronic acid (HA) and chitosan (CS) that also exhibit the tendency to form hydrogels but without micellar associations. As anticipated, the hybrid hydrogels based on HA and CS displayed negative effect and fluorescence of PF-DBT-Im was drastically quenched (Figure 5a,b) possibly due to random distribution of PF-DBT-Im molecules inside the gel network and dominating ACQ effect. In addition, other two low water dispersible CPs, that is, PF-DBT-COONa and PF-BT-Im also demonstrate formation of highly fluorescent

EIEE-active hydrogel with improved PLQY (Figure S4, Supporting Information). Finally, the constructed EIEE-active hybrid hydrogel system was utilized as a portable platform for the detection of TCs. Addition of TCs to PF-DBT-Im/Pluronic F-127 hydrogel results in transition of gel into viscous liquid at room temperature along with significant quenching of fluorescence (Figure 5c; Figures S15 and S16, Supporting Information). SEM studies also revealed the breakdown of closely-packed 3D network of hydrogel into isotopic micellar phase (Figure 5c). The concentration of TCs was also optimized (100 μM) to attain the complete breakdown of gel. The abolition of gels could be accredited to the restriction of hydrophobic interactions among the micelles through formation of multiple hydrogen bonding between TCs which consist of several –OH/NH groups and outer hydrophilic PEO section of F-127 molecules. In addition, EIEE-active hydrogel also displayed an excellent injectable property and substrate-flexibility as its casting on various substrates revealed considerable emission color (Figure 5d). Furthermore, under ambient-pressure drying, hydrogel turns into the hybrid xerogel, which also shows splendid pink color emission (Figure 5d), reflecting the nature of EIEE-active xerogel similar to AIEgens and certifying it as a solid-state hybrid fluorescent material. Thus, the ingeniously obtained EIEE-active hybrid miceller system with multiple features exhibits great prospects in the field of sensing and further studies are on the way to demonstrate its utility in enhanced photodynamic therapy and solid-state luminescent devices.

3. Conclusion

In conclusion, a new concept based on encapsulation-induced emission enhancement (EIEE) of low water dispersible CP by Pluronic micelles is presented for restraining longstanding ACQ problem, improving overall PLQY, and attaining augmented detection performance. The facile encapsulation of ACQ affected CP PF-DBT-Im inside Pluronic F-127 micelles, resulting in successful transformation into EIEE-active fluorescent hybrid micelles and hydrogel with enhanced PLQY up to ≈200% increment. EIEE-active hybrid micellar system not only showed superior photophysical properties but also demonstrated amplified detection of tetracyclines via synergistic effect of PET, IFE, and long-range rapid exciton diffusion of quencher molecules endorsing the advantage of EIEE-active hybrid material over ACQ suffered PF-DBT-Im random aggregates. Moreover, gel-to-sol transition of EIEE-active hydrogel with complete disappearance of emission color in the presence of tetracyclines endorses a convenient platform for visual and on-site detection. Finally, EIEE-active hybrid hydrogel with reasonable injection, casting property, along with astonishing emission color in dry solid state confirms its strong resemblance with AIEgens and indicates likely futuristic applications in biomedicine and solid-state optoelectronics.

4. Experimental Section

The details of synthetic methods and experimental procedures are described in the Supporting Information.

Supporting Information

Supporting Information is available from the Wiley Online Library or from the author.

Acknowledgements

Financial support from the National Natural Science Foundation of China (Nos. 81701830 and 22250410261), the Natural Science Foundation of Shaanxi Province (Nos. 2020JM-066 and 2020JQ-019), the Fundamental Research Funds for the Central Universities (Nos. xjh012020001, xjj2017028, and xjh012020011), and the China Postdoctoral Science Foundation (Nos. 2020M673368 and 2020M673428) is gratefully acknowledged. The authors also appreciate valuable discussion with Yaming Ma regarding cyclic voltammetry studies. S.H. acknowledges the Ministry of Science & Technology, China for foreign youth talent support program (No. QN2021170004L). The Instrumental Analysis Center of Xi'an Jiaotong University is acknowledged for instrument facilities.

Conflict of Interest

The authors declare no conflict of interest.

Data Availability Statement

The data that support the findings of this study are available in the supplementary material of this article.

Keywords

conjugated polymers, luminescent hybrid materials, luminescent hydrogels, optical properties, sensors

Received: November 29, 2022
Revised: February 9, 2023
Published online: April 19, 2023

[1] O. Ostroverkhova, *Chem. Rev.* **2016**, *116*, 13279.
[2] L. Zhou, F. Lv, L. Liu, S. Wang, *Acc. Chem. Res.* **2019**, *52*, 3211.
[3] P.-O. Morin, T. Bura, M. Leclerc, *Mater. Horiz.* **2016**, *3*, 11.
[4] Q. Zhou, T. M. Swager, *J. Am. Chem. Soc.* **1995**, *117*, 12593.
[5] S. W. Thomas, G. D. Joly, T. M. Swager, *Chem. Rev.* **2007**, *107*, 1339.
[6] X. Chen, S. Hussain, Y. Hao, X. Tian, R. Gao, *ECS J. Solid State Sci. Technol.* **2021**, *10*, 037006.
[7] H. Zhong, C. Liu, W. Ge, R. Sun, F. Huang, X. Wang, *ACS Appl. Mater. Interfaces* **2017**, *9*, 22875.
[8] J. Wang, F. Lv, L. Liu, Y. Ma, S. Wang, *Coord. Chem. Rev.* **2018**, *354*, 135.
[9] W. Wu, G. C. Bazan, B. Liu, *Chem* **2017**, *2*, 760.
[10] Y. Huang, J. Xing, Q. Gong, L.–C. Chen, G. Liu, C. Yao, Z. Wang, H.–L. Zhang, Z. Chen, Q. Zhang, *Nat. Commun.* **2019**, *10*, 169.
[11] S. R. Amrutha, M. Jayakannan, *J. Phys. Chem. B* **2008**, *112*, 1119.
[12] D. Wang, Y. Yuan, Y. Mardiyati, C. Bubeck, K. Koynov, *Macromolecules* **2013**, *46*, 6217.
[13] J. Luo, Z. Xie, J. W. Y. Lam, L. Cheng, H. Chen, C. Qiu, H. S. Kwok, X. Zhan, Y. Liu, D. Zhu, B. Z. Tang, *Chem. Commun.* **2001**, 1740.
[14] R. Hu, N. L. C. Leung, B. Z. Tang, *Chem. Soc. Rev.* **2014**, *43*, 4494.
[15] X. Cai, B. Liu, *Angew. Chem., Int. Ed.* **2020**, *59*, 9868.
[16] L. Xu, Z. Wang, R. Wang, L. Wang, X. He, H. Jiang, H. Tang, D. Cao, B. Z. Tang, *Angew. Chem., Int. Ed.* **2019**, *59*, 9908.

[17] T. Zhou, R. Hu, L. Wang, Y. Qiu, G. Zhang, Q. Deng, H. Zhang, P. Yin, B. Situ, C. Zhan, A. Qin, B. Z. Tang, *Angew. Chem., Int. Ed.* **2020**, *59*, 9952.
[18] F. Qiu, C. Tu, R. Wang, L. Zhu, Y. Chen, G. Tong, B. Zhu, L. He, D. Yan, X. Zhu, *Chem. Commun.* **2011**, *47*, 9678.
[19] Y. Zhang, Z. Li, Q. Sun, Z. Li, Y. Zhi, R. Nie, H. Xia, Y. Yu, X. Liu, *Macromol. Rapid Commun.* **2021**, *42*, 2100469.
[20] N. Alizadeh, A. Akbarinejad, A. Ghoorchian, *ACS Appl. Mater. Interfaces* **2016**, *8*, 24901.
[21] J. Zhang, A. Mohsin, Y. Peng, Y. Dai, Y. Zhuang, M. Guo, P. Zhao, *ACS Appl. Mater. Interfaces* **2021**, *13*, 3512.
[22] C. Zhu, L. Liu, Q. Yang, F. Lv, S. Wang, *Chem. Rev.* **2012**, *112*, 4687.
[23] L. Xu, Z. Wang, R. Wang, L. Wang, X. He, H. Jiang, H. Tang, D. Cao, B. Z. Tang, *Angew. Chem., Int. Ed.* **2020**, *59*, 9908.
[24] X. Ji, Y. Yao, J. Li, X. Yan, F. Huang, *J. Am. Chem. Soc.* **2013**, *135*, 74.
[25] E. Elmalem, F. Biedermann, M. R. J. Scherer, A. Koutsioubas, C. Toprakcioglu, G. Biffi, W. T. S. Huck, *Chem. Commun.* **2014**, *50*, 8930.
[26] H. Yuan, Y. Zhan, A. E. Rowan, C. Xing, P. H. J. Kouwer, *Angew. Chem., Int. Ed.* **2020**, *59*, 2720.
[27] T. Kai, M. Kishimoto, M. Akita, M. Yoshizawa, *Chem. Commun.* **2018**, *54*, 956.
[28] H.-G. Fu, Y. Chen, X. Y. Dai, Y. Liu, *Adv. Opt. Mater.* **2020**, *8*, 2000220.
[29] J. L. Martinez, *Environ. Pollut.* **2009**, *157*, 2893.
[30] C. Li, X. Zhang, S. Wen, R. Xiang, Y. Han, W. Tang, T. Yue, Z. Li, *J. Hazard. Mater.* **2020**, *395*, 122615.
[31] M. Lin, H. Y. Zou, T. Yang, Z. X. Liu, H. Liu, Huang, C. Z., *Nanoscale* **2016**, *8*, 2999.
[32] X.-D. Zhu, K. Zhang, Y. Wang, W.-W. Long, R.-J. Sa, T.-F. Liu, J. Lü, *Inorg. Chem.* **2018**, *57*, 1060.
[33] A. B. A. Boxall, D. W. Kolpin, B. Halling–Sørensen, J. Tolls, *Environ. Sci. Technol.* **2003**, *37*, 286A.
[34] Q.-Q. Zhang, G.-G. Ying, C.-G. Pan, Y.-S. Liu, J.-L. Zhao, *Environ. Sci. Technol.* **2015**, *49*, 6772.
[35] C. Li, W. Yang, X. Zhang, Y. Han, W. Tang, T. Yue, Z. Li, *J. Mater. Chem. C* **2020**, *8*, 2054.
[36] Y. Chen, Y. Zhang, T. Lyu, Y. Wang, X. Yang, X. Wu, *J. Mater. Chem. C* **2019**, *7*, 9241.
[37] A. H. Malik, P. K. Iyer, *ACS Appl. Mater. Interfaces* **2017**, *9*, 4433.
[38] S. Hussain, X. Chen, C. Wang, Y. Hao, X. Tian, Y. He, J. Li, M. Shahid, P. K. Iyer, R. Gao, *Anal. Chem.* **2022**, *94*, 10685.
[39] U. Chitgupi, N. Nyayapathi, J. Kim, D. Wang, B. Sun, C. Li, K. Carter, W.–C. Huang, C. Kim, J. Xia, J. F. Lovell, *Adv. Mater.* **2019**, *31*, 1902279.
[40] Y. Zhang, W. Song, J. Geng, U. Chitgupi, H. Unsal, J. Federizon, J. Rzayev, D. K. Sukumaran, P. Alexandridis, J. F. Lovell, *Nat. Commun.* **2016**, *7*, 11649.
[41] W. Huang, E. Smarsly, J. Han, M. Bender, K. Seehafer, I. Wacker, R. R. Schröder, U. H. F. Bunz, *ACS Appl. Mater. Interfaces* **2017**, *9*, 3068.
[42] X. Chen, S. Hussain, X. Chen, Y. Hao, P. Zhang, R. Gao, *Sens. Actuators, B* **2023**, *377*, 133081.
[43] C. Alvarez–Lorenzo, A. Sosnik, A. Concheiro, *Curr. Drug Targets* **2011**, *12*, 1112.
[44] L. Jiang, X. Chen, N. Lu, L. Chi, *Acc. Chem. Res.* **2014**, *47*, 3009.
[45] P. L. Donabedian, M. N. Creyer, F. A. Monge, K. S. Schanze, E. Y. Chi, D. G. Whitten, *Proc. Natl. Acad. Sci. U. S. A.* **2017**, *114*, 7278.
[46] C. Du, D. Gao, M. Gao, H. Yuan, X. Liu, B. Wang, C. Xing, *ACS Appl. Mater. Interfaces* **2021**, *13*, 27955.
[47] G. Rainò, T. Stöferle, C. Park, H.-C. Kim, I.-J. Chin, R. D. Miller, R. F. Mahrt, *Adv. Mater.* **2010**, *22*, 3681.
[48] X.–H. Jin, M. B. Price, J. R. Finnegan, C. E. Boott, J. M. Richter, A. Rao, S. M. Menke, R. H. Friend, G. R. Whittell, I. Manners, *Science* **2018**, *360*, 897.
[49] P. N. Hurter, T. A. Hatton, *Langmuir* **1992**, *8*, 1291.
[50] S.; Hussain, A. H. M., P. K. Iyer, *J. Mater. Chem. B* **2016**, *4*, 4439.
[51] M. Gilbert, B. Albinsson, *Chem. Soc. Rev.* **2015**, *44*, 845.
[52] S. Hussain, A. H. Malik, M. A. Afroz, P. K. Iyer, *Chem. Commun.* **2015**, *51*, 7207.
[53] D. Li, H. Zhang, Y. Wang, *Chem. Soc. Rev.* **2013**, *42*, 8416.
[54] L. Ying, C.-L. Ho, H. Wu, Y. Cao, W.-Y. Wong, *Adv. Mater.* **2014**, *26*, 2459.
[55] A. H. Malik, A. Kalita, P. K. Iyer, *ACS Appl. Mater. Interfaces* **2017**, *9*, 37501.
[56] S. Parola, B. Julián–López, L. D. Carlos, C. Sanchez, *Adv. Funct. Mater.* **2016**, *26*, 6506.
[57] N. Mehwish, X. Dou, Y. Zhao, C.-L. Feng, *Mater. Horiz.* **2019**, *6*, 14.
[58] Y. Li, D. J. Young, X. J. Loh, *Mater. Chem. Front.* **2019**, *3*, 1489.
[59] S. Wei, Z. Li, W. Lu, H. Liu, J. Zhang, T. Chen, B. Z. Tang, *Angew. Chem., Int. Ed.* **2021**, *60*, 8608.
[60] W. Lu, S. Wei, H. Shi, X. Le, G. Yin, T. Chen, *Aggregate* **2021**, *2*, e37.